applied sciences

MDPI

Article

Thermoforming of Non-Developable Surfaces: Challenges in the Manufacture of Solid Surfaces, the Case of Krion K-Life

Ferran Ventura Blanch *,†, Vishal Shahdadpuri Aswani † and Pablo Hernández Vílchez †

Laboratorio de Arquitectura Experimental Avanzada y Nuevas Tecnologías, Escuela Técnica Superior de Arquitectura, Universidad de Málaga, 29071 Málaga, Spain; vishal@uma.es (V.S.A.); pablohv@uma.es (P.H.V.)

* Correspondence: ferranventura@uma.es

† These authors contributed equally to this work.

Abstract: This research arises from the need to rethink children's play spaces found in the city through new manufacturing methods of solid surface materials such as Krion K-Life 1100, which allow the creation of complex ergonomic shapes. The method consisted of an iterative digital fabrication process, in which a series of molds were developed and adjusted to thermoform a solid surface material, adapting the design in each iteration according to the results obtained. Parametric digital modeling techniques and in-depth curvature analysis were carried out to optimize the geometry, in order to meet the technical limitations of the material and the manufacturing process itself. The results showed that, through precise adjustments in the curvature and thickness of the surface, it is possible to thermoform the solid surface without defects, such as folds or wrinkles, revealing it as a viable material for the generation of complex double-curved geometries, opening up a range of possibilities from the creation of new children's spaces to parametric facades optimized according to their location.

Keywords: Krion K-Life 1100; thermoforming; digital fabrication; parametric curvature analysis; innovative children's playgrounds

Academic Editor: Andrea Frazzica

Received: 30 November 2024
Revised: 20 December 2024
Accepted: 23 December 2024
Published: 2 January 2025

Citation: Ventura Blanch, F.; Shahdadpuri Aswani, V.; Hernández Vílchez, P. Thermoforming of Non-Developable Surfaces: Challenges in the Manufacture of Solid Surfaces, the Case of Krion K-Life. *Appl. Sci.* **2025**, *15*, 363. https://doi.org/10.3390/app15010363

1. Introduction

From a spatial perspective, geometric rationalization is a distinctly human construct; in nature, straight lines are rare. Traditional architecture often relies on orthogonal approaches, where spaces and paths are formed by intersecting static, perpendicular planes [1]. This geometric simplification facilitates the construction and fabrication of structural elements but can create a disconnect from natural biomimetic patterns, reducing the ergonomic and sensory richness of spatial environments.

Considering motor and psychological factors is particularly significant during the early stages of human development, when play serves as a primary learning mechanism [2]. During these formative years, it is critical to encourage less linear, more organic movements that promote asynchronous and multidirectional body motions. Environments reflecting natural forms can enhance reflexes, motor coordination, and cognitive responses, contributing to holistic human development.

Recent research underscores the importance of designing nature-based outdoor play and learning environments for children under three years old, showing that such spaces significantly impact their holistic development [3]. Incorporating natural elements and organic forms into these environments enhances sensory experiences, encourages exploration, and fosters physical, cognitive, and emotional growth [3]. This aligns with the increasing

recognition that early childhood environments should mimic natural settings to support health and learning outcomes.

In keeping with this understanding, there is a growing need to develop children's play equipment that is more closely connected to natural morphological patterns. By implementing designs that support motor development and enable early diagnosis of developmental issues, a more suitable environment for holistic child development can be achieved [4].

Creating such ergonomic geometries, especially those based on Gaussian curvature [5,6], presents significant manufacturing challenges. Traditional methods often struggle to produce double-curved surfaces and complex organic shapes. Thermoforming has emerged as a key technique for fabricating such geometries, particularly for materials that require precise control over deformation processes [7]. This process involves heating a plastic sheet to a pliable temperature, forming it over a mold, and trimming it to produce a usable product, offering efficiency and the ability to create large parts with intricate details.

Advanced modeling of the thermoforming process using thermo-visco-hyperelastic models has been explored to predict material behavior accurately during forming [7]. Factors such as temperature, pressure, and mold interaction significantly influence the thickness distribution and mechanical properties of the formed material [7,8].

Moreover, advances in thermoforming fiber-reinforced thermoplastic composites have shown promise for creating lightweight, durable structures with complex shapes [9,10]. These composites offer advantages such as recyclability, high strength-to-weight ratios, and reduced environmental impact. However, challenges remain in optimizing process parameters to avoid defects like wrinkling, thinning, and residual stresses [9,11].

In the context of outdoor children's play areas, it is essential to consider manufacturability, durability, safety, and environmental impact. Solid surface materials stand out as promising candidates due to their thermoformability, non-porosity, antibacterial properties, and resistance to external agents. The material used in this case study is composed of approximately two-thirds natural minerals and a low percentage of high-resistance resins [12]. These properties make it ideal for creating complex geometries while meeting strict safety and hygiene standards.

Previous studies have highlighted the importance of precise control in the thermoforming process to prevent defects and achieve the desired geometry [13]. Ku et al. [13] emphasized the role of mold design, heating methods, and cooling rates in successfully shaping solid surface materials into complex forms.

Advances in digital fabrication and parametric modeling have further streamlined the design and manufacturing of complex geometries [14]. Computational tools now allow for the simulation and optimization of thermoforming processes, reducing reliance on trial-and-error methods and minimizing material waste.

This study explores the use of solid surface materials for the fabrication of complex, double-curved, and durable surfaces that enable innovative play spaces.

2. Materials

The material selected for this study belongs to the Krion® family of advanced solid surfaces, developed by Systempool, a division of the Porcelanosa Group (Vila-real, Castellón, Spain). Krion products are known for their unique composition of approximately 67% natural minerals, mainly alumina trihydrate (ATH), and 33% high-strength resins. This combination provides a wide range of properties that are intrinsic to the Krion brand, making it a leading choice for applications requiring performance, hygiene, and durability [12]:

- **Thermoformability**: The material can be heated and molded into intricate shapes without compromising its mechanical properties. Optimal forming temperatures

range between 130 and 160 °C, depending on the complexity of the shape and the desired radius.

- **Non-porosity and hygiene**: It is non-porous and has proven antibacterial properties, making it suitable for environments where hygiene is paramount, such as children's play areas.
- **Mechanical strength**: Exhibiting superior mechanical performance, it achieves flexural strength values between 60 and 78 MPa and tensile strength ranging from 40 to 60 MPa, ensuring robust resistance under mechanical loads.
- **Environmental resistance**: Engineered to withstand UV radiation ($\Delta E < 1.5$ after 10 years), thermal fluctuations, and exposure to external agents, this material is well adapted for prolonged outdoor use.
- **Sustainability**: Krion is 100% recyclable and features Eco-Active Solid Technology, contributing to environmental sustainability by purifying air and easing maintenance through self-cleaning properties.

Among the Krion product range, Krion K LIFE 1100 was selected for its enhanced functionality, which surpasses not only alternative solid surfaces such as Corian but also other Krion models. This choice was driven by its exceptional performance in hygiene, sustainability, and environmental resilience.

- **Eco-Active Solid Technology**: This unique feature enables air purification and contributes to maintaining cleaner and healthier environments, making it particularly well suited for children's spaces.
- **GREENGUARD gold certification**: Achieving this stringent certification demonstrates compliance with the highest standards for low chemical emissions, ensuring improved indoor air quality, particularly in sensitive environments such as nurseries and healthcare facilities.
- **Antiviral properties**: Studies conducted by Virology Research Services Ltd. (Sittingbourne, UK), using a modified ISO 21702 protocol [15], demonstrated the superior antiviral performance of the selected material, achieving an 82.22% reduction in infectivity of human coronavirus NL63 within 24 h (compared to 55.28% on plastic) and an 88.75% reduction in infectivity of the Influenza A virus within 2 h (compared to 18.44% on plastic). These properties make it an ideal choice for environments with high sanitary demands, supporting the creation of ergonomic and hygienic double-curved surfaces for children's play areas.

2.1. Mechanical Properties and Thermoforming Characteristics

A summary of these properties is presented in Table 1.

Table 1. Mechanical properties and thermoforming characteristics of Krion® K-Life 1100 [12].

Property	Value/Range	Unit
Density	1.71–1.77	g/cm^3
Flexural Strength	60–78	MPa
Flexural Modulus	8500–11,900	MPa
Tensile Strength	40–60	MPa
Elongation at Break	0.7–0.85	%
Compression Strength	97–117	MPa
Hardness (Barcol)	60–65	Barcol Units
Thermal Conductivity (λ)	0.396	W/m·K

Table 1. *Cont.*

Property	Value/Range	Unit
Thermal Expansion Coefficient	3.5×10^{-5}	mm/m·°C
Water Absorption	0.03	%
UV Resistance	$\Delta E < 1.5$ (after 10 years)	—
Fire Classification	B s1 d0	Euroclass

2.2. Thermoforming Capabilities

Achieving the minimal radius without defects is a critical factor in thermoforming solid surfaces. Factors influencing the minimal thermoforming radius include [12] the following:

- **Sheet thickness**: Thicker sheets, like the 12 mm sheet used in this study, require larger radii to avoid excessive stress. According to the manufacturer's specifications, the minimal interior radius achievable with thermoforming for a 12 mm thick Krion sheet is 20 mm [12] under optimal conditions. However, without heating (cold bending), the material requires a minimum radius of 1800 mm for 12 mm thick sheets, restricting the allowable outcomes when shaping at room temperature.
- **Temperature control**: Precise temperature control ensures the material reaches a pliable state without degrading.
- **Forming pressure**: Uniform and sufficient pressure during forming helps the material conform to the mold without introducing defects.
- **Mold design and quality**: Smooth and accurately designed molds reduce the likelihood of surface imperfections and ensure the material forms correctly.
- **Heating uniformity**: Ensuring an even preheating of the sheet to the required temperature range is essential to prevent an irregular stress distribution that could lead to defects like cracking or warping.

2.3. Comparison with Other Materials

The selected material must not only enable the fabrication of intricate geometries but also adhere to stringent standards of safety, durability, hygiene, and environmental sustainability. Unlike single-curvature geometries such as cylinders or cones, which can be unrolled onto planar surfaces without significant distortion, double-curvature geometries present inherent challenges due to their non-developable nature. These surfaces cannot be flattened into a two-dimensional plane without introducing deviations or tolerances, often necessitating material adjustments such as stretching, warping, or localized deformation to achieve the desired form. This characteristic places additional demands on the starting material, which must exhibit the flexibility and mechanical properties required to accommodate these deformations while maintaining structural integrity. Traditional materials such as wood, metal, glass, and conventional plastics offer distinct advantages but are often constrained by their inability to meet these complex manufacturing requirements within this highly specialized context.

- **Wood:** This is a common material for playground equipment, valued for its natural aesthetic and ease of fabrication. Techniques such as steam bending and laminating allow some flexibility in shaping wood for curved applications. Nonetheless, it is prone to environmental degradation, including rot, warping, and insect infestation, which can compromise both safety and durability. Its porous surface also presents hygiene challenges, as it can harbor bacteria and fungi, posing potential health risks in environments designed for children [16].
- **Metal:** Metals provide exceptional strength and durability, making them popular choices for playground equipment. On the other hand, their application in

complex, double-curved geometries is limited due to the need for specialized and costly fabrication techniques, such as metal stamping, incremental sheet forming, or hydroforming [17]. Metal surfaces also present safety risks in outdoor environments, as they can become excessively hot or cold, potentially causing burns or discomfort. Additionally, susceptibility to corrosion requires regular maintenance to ensure structural integrity and prevent failures [17].

- **Glass:** Although it can be molded into complex forms using techniques like slumping or bending, glass is generally unsuitable for playground equipment due to its inherent brittleness and the risk of breakage, which presents significant safety concerns. Even tempered or laminated glass, while stronger and less prone to fragmentation, can still shatter under impact, making it an impractical choice for environments designed for children [18].
- **Conventional plastics and composites:** Widely used in playgrounds due to their moldability and lower cost, conventional plastics can be shaped into intricate designs through methods such as thermoforming or injection molding. Nevertheless, they often fall short in terms of mechanical strength and UV resistance, limiting their durability in outdoor applications. Prolonged exposure to sunlight can lead to degradation, resulting in brittleness and potential breakage. Environmental concerns also arise from the non-recyclable nature of certain plastics and the release of microplastics into the environment [19]. Fiber-reinforced composites offer enhanced strength and durability, but challenges such as wrinkling or residual stresses during fabrication can adversely impact both structural integrity and aesthetic quality [20].

In summary, while traditional materials such as wood, metal, glass, and conventional plastics each have specific advantages, they present significant limitations for the design and fabrication of complex, double-curved surfaces in children's playground equipment.

3. Methods

This study centers on the characterization of a solid surface material, with a thickness of 12 mm, aimed at developing a crawling surface for outdoor children's play areas. To achieve this objective, an iterative manufacturing process was implemented, tailored to the material's specific requirements [13]. This process comprised four distinct phases, as outlined in Figure 1.

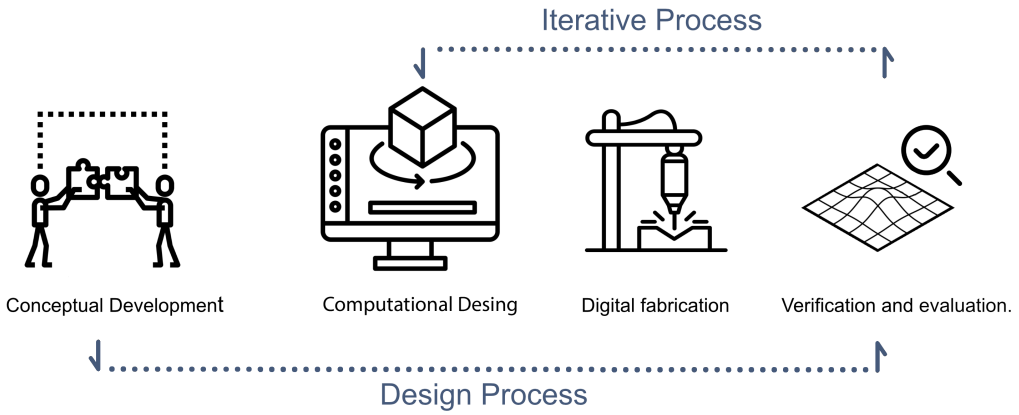

Figure 1. Functional diagram of the workflow developed during the manufacturing process.

3.1. Conceptual Development

This phase involved the preliminary analysis and initial development of ideas and solutions. The project began with an in-depth study of how children interact with play spaces in urban environments, emphasizing the role of spatial design in influencing physi-

cal and cognitive development. To adopt a comprehensive and multidisciplinary approach, the team collaborated with professionals including child psychologists, educators, and ergonomics experts. Their expertise was instrumental in recognizing the importance of organic forms and ergonomic shapes in fostering natural movement and sensory engagement. Brainstorming sessions and workshops were conducted to gather diverse perspectives and identify key features that enhance play and development. This collaborative effort culminated in the conceptualization of a complex, modular surface designed with the goal of promoting creativity, motor skills, and social interaction within a safe and stimulating environment (Figure 2).

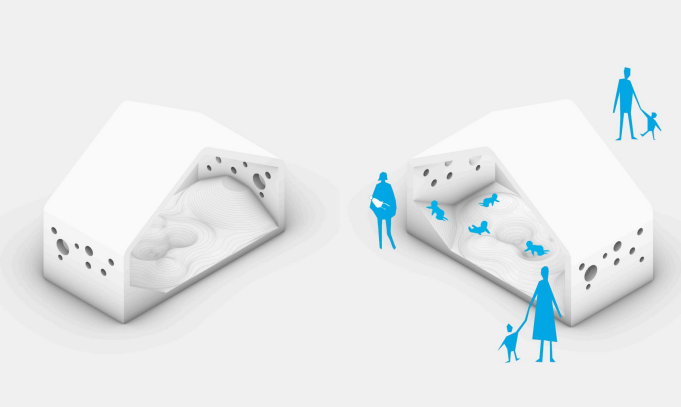

Figure 2. Original concept of the architectural space to be achieved. The layout and container spaces were maintained, while the crawling design underwent modifications due to the findings of this research.

3.2. Computational Design and Feasibility

The objective of this stage was to define the processes and methods necessary for the creation of the surface, encompassing material selection and the generation of a digital fabrication twin tailored to the constraints imposed by both the material and the production system.

A parametric design approach was utilized, employing the Rhinoceros computer-aided design software (Rhino v6.35) and the Grasshopper visual programming environment (Grasshopper v1.0). This methodology facilitated the development of an iterative and optimizable digital model, refined based on results obtained throughout the process.

The base model was a horizontal surface measuring 1800 mm × 3750 mm, with deviations applied along the Z-axis to introduce the desired dynamic and varied forms. Subsequently, the geometry was adjusted to accommodate technical manufacturing constraints. Specifically, to align with available machinery and optimize the use of high-cost material, the surface was subdivided into five modules measuring 1800 mm × 750 mm, optimizing the original Krion panel dimensions of 3660 mm × 760 mm.

For sustainability purposes, the geometry was further rationalized to achieve a similar result without requiring the production of five separate molds. This refinement resulted in the development of two distinct modules: one designed as an end piece and the other to form the remaining four segments. The ends of these modules were adapted to interlock seamlessly, enabling the complete surface to be constructed by repeating the same module while applying rotational and translational movements (Figure 3).

Finally, a detailed Gaussian analysis of the obtained curvature and minimum manufacturing radius was performed using the Rhino software. This analysis consists of evaluating the curvature of the surface to identify areas that may present problems during fabrication [14]. In Rhino, the Gaussian curvature analysis function is used to visualize how the curvature varies along the surface.

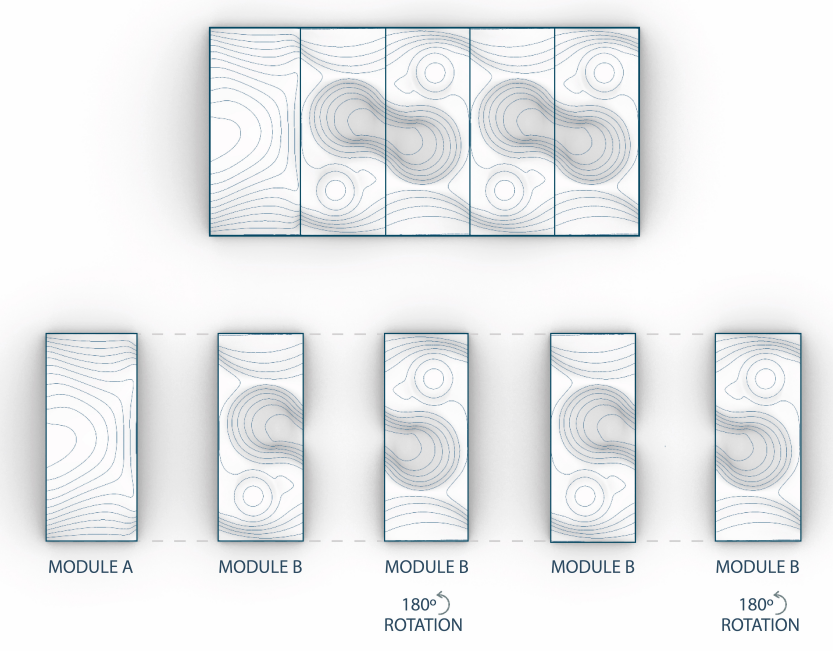

Figure 3. Modulation and splitting strategy to minimize the usage of molds, and yet obtain the initial topography requirement and goals for children's motor and cognitive development.

The Gaussian curvature K at each point of the surface is calculated by the formula [21]:

$$K = k_1 \times k_2 \tag{1}$$

where k_1 and k_2 are the principal curvatures at that point. These principal curvatures represent the maximum and minimum values of the normal curvature in all possible directions at a given point on the surface. Mathematically, they are defined through a differential analysis of surfaces.

For a surface parameterized by a vector function $\mathbf{r}(u, v)$, the principal curvatures are obtained by solving the characteristic equation of the operator of form (also known as the second fundamental) [22]:

$$\det\left(\begin{pmatrix} L & M \\ M & N \end{pmatrix} - k\begin{pmatrix} E & F \\ F & G \end{pmatrix}\right) = 0 \tag{2}$$

where

- E, F, G are the coefficients of the first fundamental form, defined as [22]:

$$E = \mathbf{r}_u \cdot \mathbf{r}_u,$$
$$F = \mathbf{r}_u \cdot \mathbf{r}_v,$$
$$G = \mathbf{r}_v \cdot \mathbf{r}_v.$$

- L, M, N are the coefficients of the second fundamental form, defined as [23]:

$$L = \mathbf{r}_{uu} \cdot \mathbf{n},$$
$$M = \mathbf{r}_{uv} \cdot \mathbf{n},$$
$$N = \mathbf{r}_{vv} \cdot \mathbf{n}.$$

- $\mathbf{r}_u$ y $\mathbf{r}_v$ are the partial derivatives of $\mathbf{r}$ with respect to u and v.

- $\mathbf{n}$ is the unit normal vector to the surface, defined as [24]:

$$\mathbf{n} = \frac{\mathbf{r}_u \times \mathbf{r}_v}{\|\mathbf{r}_u \times \mathbf{r}_v\|}.$$

By solving the characteristic equation, we obtained the principal curvatures k_1 and k_2 for the surfaces under study. These values allowed us to determine the curvature in specific directions and were essential for understanding how the surface curves at each point.

Using the advanced analytical tools available in the Rhino software [6], color-coded maps can be generated to highlight areas of varying curvature intensity. These visual representations facilitate the identification of regions where curvature exceeds the material's allowable thresholds, potentially leading to issues such as material failure or deformation during the thermoforming process. This proactive approach optimizes the surface design prior to physical fabrication, minimizing the risk of defects and ensuring that the final product retains both its aesthetic appeal and structural integrity.

The model was analyzed within a curvature range oscillating between $4.73\,\mathrm{m}^{-2}$ and $-4.73\,\mathrm{m}^{-2}$ Figure 4. This process enabled detailed visualization and precise quantification of curvature variations across the entire surface, which was crucial for ensuring that the design adhered to the mechanical and physical limits of the solid surface material.

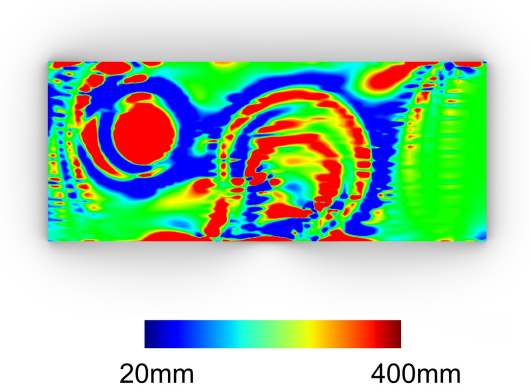

Figure 4. Gaussian analysis of module B conducted within the curvature range oscillating between $4.73\,\mathrm{m}^{-2}$ and $-4.73\,\mathrm{m}^{-2}$ using the Rhino3D analysis tools.

Studies on composite laminates similar to Krion [10], particularly thermoformable polymers, have shown that even minor angular deviations in the design can induce significant residual stresses during the forming process [11]. These residual stresses can result in unwanted deformations, such as warping or buckling, and alter the intended angles in sections designed to meet specific geometric criteria. Such deformations not only impact the visual quality of the final product but may also compromise its structural performance and safety—key considerations in applications such as children's playground equipment. For this reason, meticulous control of curvature and topology during the design phase is essential. This involves careful planning of surface geometry, detailed stress distribution analyses, and iterative adjustments to the design to mitigate potential issues. By following this approach, structural problems during manufacturing can be avoided, ensuring that the final product meets all functional requirements, adheres to safety standards, and delivers the intended aesthetic experience.

3.3. Digital Fabrication

During this phase, all necessary processes were executed to materialize the projected design. The solid surface, being thermoformable, can be adapted to different geometries through the controlled application of heat and pressure. The influence of these factors

has been already studied in the behavior of polymeric composites [8], underscoring the importance of precise control to prevent defects such as wrinkles and folds.

To apply the appropriate pressure during the thermoforming process, a wooden mold was developed to act as a negative. This was achieved using computer numerical control (CNC) machines, ensuring the material's intended shape was accurately reproduced.

The mold was fabricated using medium-density fiberboard (MDF) recycled from the laboratory, which helped reduce both costs and the environmental impact of the project. A high-precision TEC-CAM 1103 3-axis CNC router machine (PEREZ-CAMPS, Viladecans, Barcelona, Spain) was employed for cutting and roughing the boards.

The process began with an initial approximation of the geometry through the stacking of recut MDF boards into simple rectangular shapes, minimizing material waste, processing time, and the number of machining passes compared to using a solid wood block. The laminated boards were then subjected to roughing passes to refine the geometry in line with the digital model. Finally, a finishing pass was performed to produce a continuous, smooth surface, free from irregularities or abrupt variations (Figures 5 and 6).

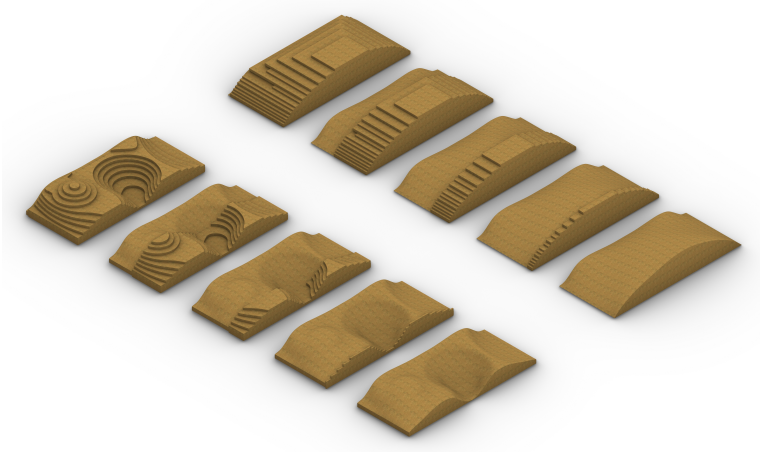

Figure 5. Fabrication process of the MDF molds, from the original stack of cut leftovers (**left**) to the final sanded piece (**right**). Unique module A (**top**) and repetitive module B (**bottom**).

Once the mold was fabricated, it was placed in the thermoforming machine. For this process, the Global Duo Standard from Global Vacuum was utilized. The material was heated to 160° for 22 min to achieve the desired shape, followed by an additional 40 min in the heat chamber to ensure proper formation (Figure 7). The temperatures and heating times were adjusted in order to minimize the appearance of residual stresses, in accordance with the manufacturer's specifications [25], which are primarily designed for single-curvature applications. The only modification to these specifications was based on the thickness of the sheet. The base heating time was 10 min, with an additional minute added for each millimeter of thickness. These specifications were also slightly increased to accommodate the demands of double-curvature operations. Only a base mold was used, eliminating the need for a counter-mold. This approach significantly streamlined production, made possible by the optimized geometry and the use of a membrane press within the heated chamber.

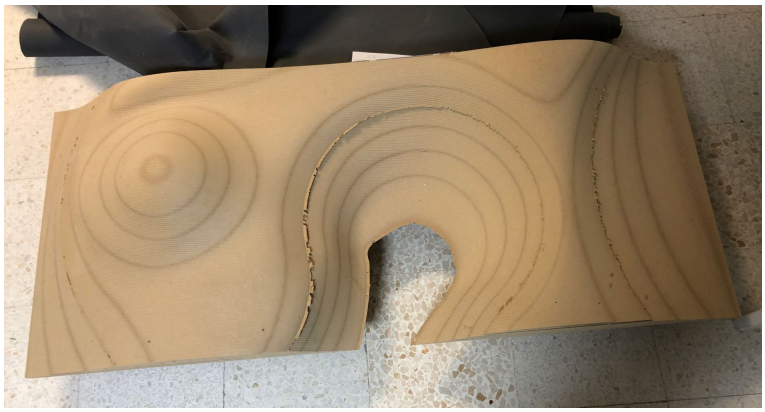

Figure 6. Actual fabricated MDF mold of module B: first iteration, before sanding. The piece was later modified and processed with filler to accomplish the changes required to obtain the final installed piece.

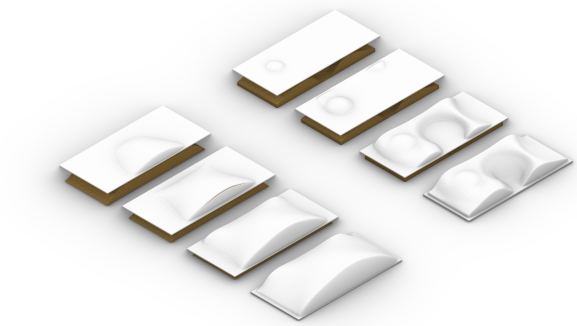

Figure 7. Initial digital simulation of the thermoforming process performed in Grasshopper to check the viability of the design. This was later adjusted with corrected parameters for the material constraints.

3.4. Verification and Evaluation

An exhaustive visual inspection was conducted (Figure 8) to identify anomalies such as folds, wrinkles, or surface irregularities that occurred during the thermoforming process. This preliminary evaluation played a pivotal role in detecting immediate defects that could compromise the functionality, safety, or aesthetic value of the final product. Specific regions were identified where the material's output deviated from expected behavior, providing key insights into its performance under the applied thermoforming conditions.

To enhance the precision and depth of this evaluation, a high-resolution laser scanner (FARO Focus3D X330 HDR, Lake Mary, FL, USA) was employed, generating a comprehensive point cloud dataset (Figure 9) of the piece. This process created an accurate digital twin of the physical part, capturing intricate geometric details that might escape visual detection. The resulting data were subsequently processed using specialized software (FARO SCENE_2018.0.0.648), allowing for a detailed comparison between the scanned geometry and the original CAD model. This overlay analysis facilitated the identification of subtle discrepancies in curvature, dimensions, and surface continuity. Such insights enabled the team to correlate the material properties and process parameters with observed geometric deviations, guiding informed adjustments to both the design and manufacturing workflows.

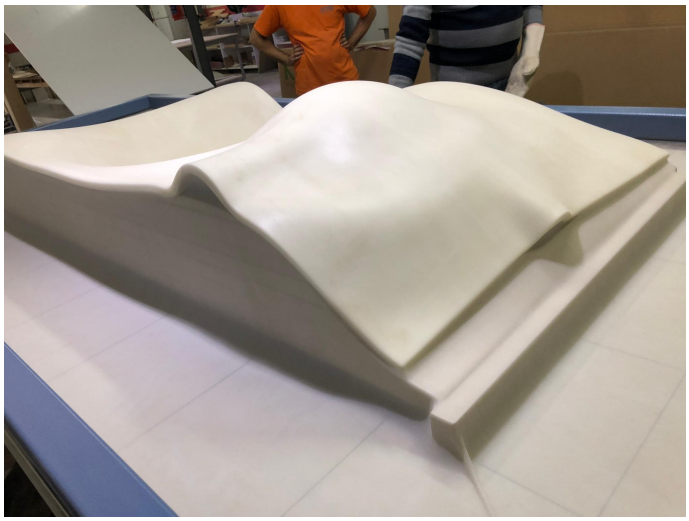

Figure 8. Wrinkles and folds appeared in the first full prototype and process testing, not achieving the expected output. Data collected before, during, and after the thermoforming influenced the next (successful) iterations.

This cross-check provided a detailed understanding of the material and process-induced tolerances, revealing regions where the material exhibited excessive stretching or compression, resulting in undesirable variations such as thinning or thickening, which could compromise structural integrity. Additionally, stresses and distortions accumulated during the cooling phase were determined to be key challenges that must be carefully controlled to ensure the durability and safety of the final product.

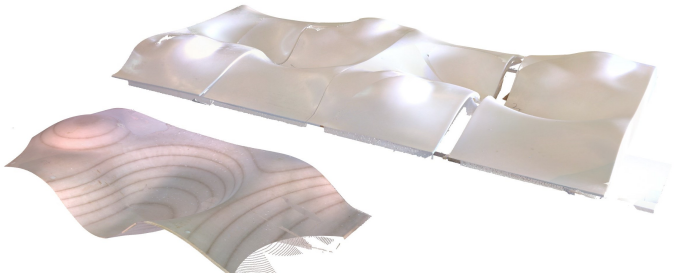

Figure 9. Point cloud mesh result of 3D laser scanning used to compare the desired and obtained thermoformed modules

As highlighted in Figure 8, visible creases and deformations were present on the surface of the initial thermoforming trial, particularly in regions featuring complex double curvatures. The material's limitations in conforming to tight radii without structural compromise manifested as buckling or folding. This observation emphasized the need to balance design aesthetics and ergonomics with material and manufacturing constraints. Recognizing the relationship between excessive curvature and material failure enabled the team to adjust the design strategically, mitigating similar issues in subsequent iterations.

To address these challenges and enhance the manufacturing process while maintaining a focus on sustainability and resource efficiency, the decision was made to rework the existing mold instead of creating a new one. This approach not only reduced material waste and costs but also aligned with the project's environmental objectives by minimizing the use of additional resources. Reworking the mold involved adding filler material to convex areas to reduce excessive curvature and performing roughing and sanding on concave areas to smooth abrupt transitions and increase radii where necessary. This precise modification process, guided by curvature analyses, enabled the mold to better accommodate the material's thermoforming capabilities.

Careful planning and execution were crucial to avoid introducing new issues or endangering other design elements. The retopology of the surface was performed using mesh smoothing techniques in Rhino. This involved reorganizing and optimizing the network of polygons that defines the surface geometry to enhance its structural and visual characteristics. Refining the network eliminated irregularities, such as uneven polygon sizes, twisted faces, or unnecessary vertices, that could compromise the smoothness of the surface. Mesh smoothing helped to distribute curvature more uniformly, reducing areas of high stress concentration that could lead to deformations or failures during manufacturing. This process not only enhanced the visual fluidity of the geometry but also ensured a more predictable and stable behavior of the material under heat and pressure during thermoforming. Maintaining the curvature within allowable thresholds was required for preserving material integrity while achieving the desired ergonomic and aesthetic outcomes. Equally, the filler materials used had to be compatible with the mold's base material to maintain structural stability under the pressures and temperatures of thermoforming. Furthermore, the modified mold surfaces were meticulously sanded and finished to have the smoothness required for high-quality surface reproduction in the final product.

The iterative modifications effectively eliminated defects such as folds and wrinkles, enhancing structural integrity, visual appeal, and long-term durability.

The developed modular, stone-like surface (Figure 10) was successfully integrated into the play space and activity container. The modules were designed for efficient on-site assembly, featuring precise alignment elements to guarantee seamless connections between pieces. On-site post-processing included sanding, filling, and polishing the assembly seams to create a continuous, aesthetically pleasing surface that met both safety standards and design objectives.

Figure 10. Assembly of 4 pieces of module B, composing the integrated modular part of the installed crawling area. Module A, not present, would attach to the left side.

The design offered additional benefits, including ease of transportation, flexibility in installation, and adaptability for various play environments. By rearranging or rotating the modules, different shapes and spatial experiences could be generated, enhancing the playground's versatility and appeal. As shown in Figure 10, rotating the same piece by 180 degrees provided varied configurations, sustaining children's interest and engagement by fostering dynamic and stimulating play environments.

4. Results

A comprehensive analysis of Gaussian curvature (Figure 11) and radius (Figure 12) provided valuable insights into the thermoforming behavior, highlighting a direct correlation between surface curvature parameters and the occurrence of defects, such as folds and wrinkles, during manufacturing. These defects were particularly prevalent in areas of double curvature with radii smaller than 60 mm, underscoring the material's limitations in accommodating tight curvatures in complex geometries. While the manufacturer's specifications for Krion K-Life 1100 [25], such as a minimum interior radius of 20 mm for a 12 mm thick sheet, adequately address single-curvature surfaces, they do not fully account for the material's performance under double curvature, where simultaneous bending in two perpendicular directions imposes greater stress. Our findings further demonstrate that, while the material supports minimum radii of 20–40 mm for single-curvature surfaces without significant risk of defects, transitioning to double-curvature surfaces requires larger radii of 45–80 mm to maintain structural integrity and prevent material failure. These limitations arise from the additional stresses generated during multidirectional deformation, which exceed the material's capacity at smaller radii.

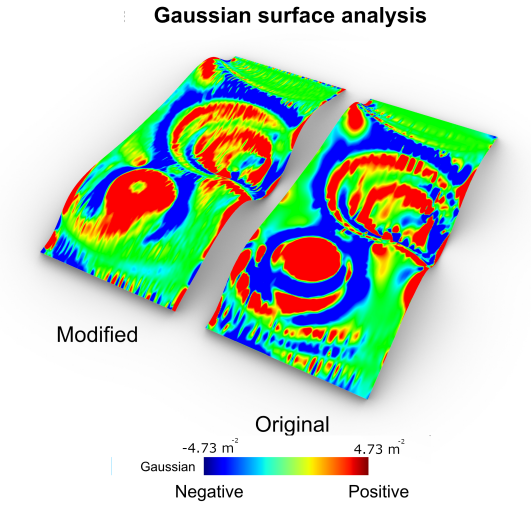

Figure 11. Comparative Gaussian analysis of module B showing the evolution of the surface between the first and last iteration.

This iterative process of analysis and modification highlighted the necessity of maintaining consistent cross-sections and carefully controlling curvature to preserve structural and load-bearing capabilities. It was determined that a minimum thickness of 10.8 mm was essential (Figure 12), ensuring a maximum material loss of only 10% in the most critical areas while maintaining strength and durability. Adhering to these parameters allowed the material to endure the stresses of thermoforming without developing thin spots or weaknesses that could compromise its performance under load [25].

The results significantly enhance the understanding and application of Krion K-Life 1100, broadening the scope of possibilities achievable with this solid surface material. By rigorously examining its thermoformable properties, its feasibility for producing complex, double-curved surfaces that were once deemed challenging or impractical with conventional materials has been proved. The successful fabrication of these intricate geometries highlights its potential not only for specialized uses, but also for broader architectural and design contexts where complex forms are desired and needed.

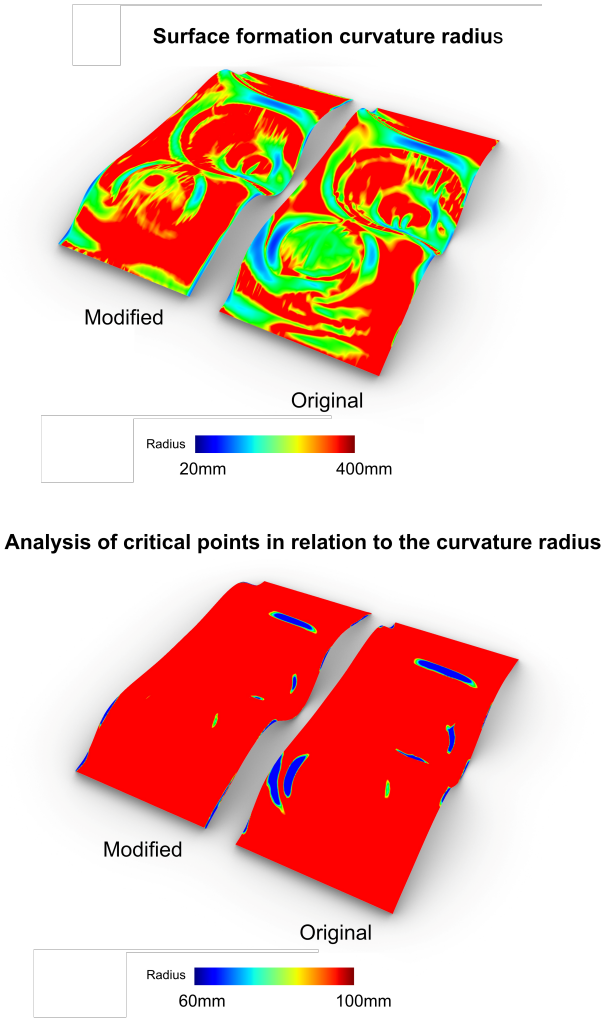

Figure 12. Comparative topological analysis of the curvature and radius of module B between the first and last iteration.

5. Conclusions

The integration of material properties with an iterative digital design and manufacturing process was instrumental in achieving these outcomes. Parametric modeling techniques provided precise control over surface geometry, enabling us to refine designs in response to the material's limitations and the manufacturing constraints encountered during fabrication. This collaboration between digital design and material science facilitated the creation of crawling surfaces that are not only visually striking but also meet rigorous functional and safety standards.

Following the implementation of changes and a comprehensive retopologization of the surface, the curvature distribution was significantly improved, resulting in a more uniform curvature profile with smoother transitions. This refinement reduced the number of critical points where curvature exceeded the material's allowable limits, minimizing high-stress areas and enhancing the manufacturability of the design. These improvements facilitated a more reliable thermoforming process while also improving the structural integrity and aesthetic quality of the final product. A comparison of Gaussian analyses between the original and modified models (Figure 11) further highlighted a clear correlation between zones of high stress and the locations where folds and wrinkles occurred during initial fabrication attempts. In the original model, dramatic fluctuations in curvature intensity, marked by pronounced transitions between positive and negative curvatures, created singular points of excessive stress during thermoforming. These sharp variations increased

the risk of defects such as folds, wrinkles, and even material failure, underscoring the importance of optimizing curvature distribution to achieve a functional and high-quality final design.

These findings are vital for the practical application of solid surfaces in complex shapes. Designers must account for these limitations when creating double-curved surfaces to ensure the material can be formed without compromising its mechanical properties. This may necessitate adjustments to curvature, alternative geometries, or the adoption of advanced fabrication techniques to address these constraints. Understanding the relationship between surface topology and material behavior fosters more effective collaboration between designers and manufacturers, also resulting in superior outcomes in both aesthetics and functionality as stated previously.

This integration of advanced digital analysis with manufacturing pragmatism underscored the value of a synergistic approach. The comprehensive refinements ensured that the final design was manufacturable while meeting the project's goals for innovative children's play spaces. By combining high-resolution laser scanning, meticulous analytical techniques, and iterative design optimization, a benchmark for the application of Krion in complex geometries was achieved. This project highlights the importance of integrating material science, digital modeling, and sustainable practices to develop innovative architectural solutions that meet functional requirements while addressing environmental responsibilities.

Overall, the successful fabrication and implementation of the modular surface validate the potential of solid surfaces for creating complex, double-curved geometries suitable for children's playgrounds. These modules aim to redefine children's interaction with their surroundings and revolutionize the design of playground equipment (Figure 13).

Figure 13. Proyecto Smart City Kids. Motor and cognitive development area. The finished unified pieces of the present research constitute the crawling surface, already open to the public.

Author Contributions: Conceptualization, F.V.B. and V.S.A.; methodology, V.S.A.; software, V.S.A.; validation, F.V.B. and V.S.A.; formal analysis, F.V.B. and V.S.A.; investigation, P.H.V.; resources, P.H.V. and V.S.A.; data curation, V.S.A. and P.H.V.; writing—original draft preparation, P.H.V. , V.S.A. and F.V.B.; writing—review and editing, P.H.V.; visualization, P.H.V. supervision, F.V.B. and V.S.A.; project administration, F.V.B.; funding acquisition, F.V.B. All authors have read and agreed to the published version of the manuscript.

Funding: This research was funded by Proyecto Smart City Kids [I Plan Propio de Smart-Campus] and Ayudas para proyectos puente [II Plan Propio de Smart-Campus]. The APC was funded by Ayudas para proyectos puente [II Plan Propio de Smart-Campus].

Institutional Review Board Statement: Not applicable.

Informed Consent Statement: Not applicable.

Data Availability Statement: The original contributions presented in this study are included in the article. Further inquiries can be directed to the corresponding author.

Acknowledgments: The authors would like to express their sincere gratitude to Nerea Salas Martín, Candela García Huber, and Raúl Ruiz Alaminos for their support in various phases of the design and their contribution in preparing several schematics. Special thanks to Fernando Alda Calvo for the photography of the project.

Conflicts of Interest: The authors declare no conflicts of interest.

Abbreviation

The following abbreviation are used in this manuscript:

CNC	Computer numerical control

References

1. Parent, C.; Virilio, P. *The Function of the Oblique: The Architecture of Claude Parent and Paul Virilio, 1963–1969*; Architectural Association: London, UK, 1996.
2. Gil Madrona, P.; Contreras Jordán, O.R.; Gómez Barreto, I. Habilidades motrices en la infancia y su desarrollo desde una educación física animada. *Rev. Iberoam. Educ.* **2008**, *47*, 71–96. [CrossRef]
3. Craig, D.; Trina, N.; Monsur, M.; Haque, U.; Farrow, G.; Hasan, M.; Tasnim, F.; Akinbobola, M. Effective Nature-Based Outdoor Play and Learning Environments for below-3 Children: A Literature-Based Summary. *Int. J. Environ. Res. Public Health* **2024**, *21*, 1247. [CrossRef] [PubMed]
4. Blanch, F.V.; Martín, N.S. Architecture and Educational Spaces for Children 0–3 as Learning Environments. *Rev. GestãO Soc. Ambient.* **2024**, *18*, e09407. [CrossRef]
5. Zhu, Y. A Study on Characteristic Line of Auto Modeling Based on Rhinoceros. *Appl. Mech. Mater.* **2012**, *184–185*, 41–44. [CrossRef]
6. Sulpizio, C.; Fiore, A.; Demartino, C.; Vanzi, I.; Briseghella, B. Optimal design criteria for form-finding of double-curved surfaces. *Procedia Manuf.* **2020**, *44*, 28–35. [CrossRef]
7. Hwang, S.F.; Yang, C.Y.; Huang, S.H. Effects of Thermoforming Parameters on Woven Carbon Fiber Thermoplastic Composites. *Materials* **2024**, *17*, 3932. [CrossRef] [PubMed]
8. Ren, Y.; Li, Z.; Li, X.; Su, J.; Li, Y.; Gao, Y.; Zhou, J.; Ji, C.; Zhu, S.; Yu, M. The Influence of Thermal Parameters on the Self-Nucleation Behavior of Polyphenylene Sulfide (PPS) during Secondary Thermoforming. *Materials* **2024**, *17*, 890. [CrossRef] [PubMed]
9. Puglia, D.; Biagiotti, J.; Kenny, J.M. A Review on Natural Fiber Based Composites Part II: Application of Natural Reinforcements in Composite Materials. *J. Nat. Fibers* **2004**, *1*, 23–65. [CrossRef]
10. Maria, F.; Pelin, C.; Pelin, G.; Rusu, B.; Stefan, A.; Stelescu, M.; Ignat, M.; Gurau, D.; Georgescu, M.; Nituica (Vilsan), M.; et al. Development, Testing, and Thermoforming of Thermoplastics Reinforced with Surface-Modified Aramid Fibers for Cover of Electronic Parts in Small Unmanned Aerial Vehicles Using 3D-Printed Molds. *Polymers* **2024**, *16*, 2136. [CrossRef] [PubMed]
11. Hwang, S.F. An Overview of Angle Deviations of Fiber-Reinforced Polymer Composite Angular Laminates. *Materials* **2023**, *16*, 4844. [CrossRef] [PubMed]
12. Systempool. KRION® K-LIFE 1100 EAST®—Ficha de Especificación, 2023. In *Ficha Técnica con Información Sobre las Propiedades Fotocatalíticas, Mecánicas y de Diseó del Material KRION®*; Systempool: Castellón, Spain, 2023.
13. Ku, K.; Gurjar, S. Prototyping Method for Complex-Shaped Textile Composite Panels—Developing a Digitally Controlled Reconfigurable Mold. 01 2018. pp. 47–52. Available online: https://papers.cumincad.org/data/works/att/eCAADe_2018_volume2_screen_lowres_SCOPUS.pdf#page=61 (accessed on 1 May 2023).
14. du Peloux, L.; Baverel, O.; Caron, J.F.; Tayeb, F. *From Shape to Shell: A Design Tool to Materialize Freeform Shapes Using Gridshell Structures*; Design Modelling Symposium Berlin: Berlin, Germany, 2013.
15. *ISO 21702:2019*; Measurement of Antiviral Activity on Plastics and Other Non-Porous Surfaces. ISO: Geneva, Switzerland, 2019.
16. Charpentier-Alfaro, C.; Benavides-Hernández, J.; Poggerini, M.; Crisci, A.; Mele, G.; Della Rocca, G.; Emiliani, G.; Frascella, A.; Torrigiani, T.; Palanti, S. Wood-Decaying Fungi: From Timber Degradation to Sustainable Insulating Biomaterials Production. *Materials* **2023**, *16*, 3547. [CrossRef] [PubMed]

17. Jeswiet, J.; Geiger, M.; Engel, U.; Kleiner, M.; Schikorra, M.; Duflou, J.; Neugebauer, R.; Bariani, P.; Bruschi, S. Metal forming progress since 2000. *CIRP J. Manuf. Sci. Technol.* **2008**, *1*, 2–17. [CrossRef]
18. Eversmann, P.; Ihde, A.; Louter, C. Low Cost Double Curvature—Exploratory Computational Modelling, FE-analysis and Prototyping of Cold-Bent Glass. In Proceedings of the Challenging Glass 5—Conference on Architectural and Structural Applications of Glass, Ghent, Belgium, 16–17 June 2016.
19. Rabek, J.F. *Polymer Photodegradation*, 1st ed.; Springer Book Archive, Springer: Dordrecht, Switzerland, 1994; pp. XVI, 664. [CrossRef]
20. Wong, J.; Altassan, A.; Rosen, D.W. Additive manufacturing of fiber-reinforced polymer composites: A technical review and status of design methodologies. *Compos. Part B Eng.* **2023**, *255*, 110603. [CrossRef]
21. Gauss, C.F. *Disquisitiones Generales Circa Superficies Curvas*; Dietrich: Göttingen, Germany, 1827.
22. Eisenhart, L.P. *Introduction to Differential Geometry*; Princeton University Press: Princeton, NJ, USA, 1997.
23. do Carmo, M.P. *Differential Geometry of Curves and Surfaces*; Prentice-Hall: Upper Saddle River, NJ, USA, 1976.
24. Gray, A. *Modern Differential Geometry of Curves and Surfaces with Mathematica*, 3rd ed.; CRC Press: Boca Raton, FL, USA, 2006.
25. Systempool. *Catálogo General de KRION: Propiedades, Aplicaciones y Características*; Grupo Porcelanosa: Villarreal, Spain, 2016; Accedido desde documento interno.